



Next-generation models and genetic therapies for rare neuromuscular diseases  
Grant agreement No. 101080690

## **D1.1 – Generation of advanced disease-specific 3D muscle models**

Lead partner	UCL
Other contributors	BIOND, KCL

Dissemination level	Public (PU)
Contractual date of delivery	M12, 31/05/2024
Actual date of delivery	M13, 05/06/2024
Work Package	WP1
Type	Report
Version	V1.0



Funded by the **European Union**. Views and opinions expressed are however those of the author(s) only and do not necessarily reflect those of the European Union and HADEA. Neither the European Union nor the granting authority can be held responsible for them.



This work is funded by **UK Research and Innovation (UKRI)** under the UK government's Horizon Europe funding guarantee grant numbers 10080927, 10079726, 10082354 and 10078461.



This work has received funding from the **Swiss State Secretariat for Education, Research and Innovation (SERI)**

## Copyright

© Copyright 2024 MAGIC Consortium consisting of:

1. Institut National de la Sante et de la Recherche Medicale (INSERM), France
2. Medizinische Hochschule Hannover (MHH), Germany
3. Université Paris XII Val de Marne (UPEC), France
4. Children's Hospital Medical Center (CCHMC), USA
5. National University of Ireland Maynooth (NUIM), Ireland
6. Parent Project aps (PP), Italy
7. BIOND Solutions BV (BIOND), Netherlands
8. Stichting Duchenne Data Foundation (DDF), Netherlands
9. VIVEbiotech sl (VIVE), Spain
10. ReiThera srl (RT), Italy
11. Siegfried DiNAMIQS (DNMQS), Switzerland
12. The Francis Crick Institute Limited (CRICK), UK
13. King's College London (KCL), UK
14. Muscular Dystrophy Group of Great Britain and Northern Ireland (MDUK), UK
15. University College London (UCL), UK
16. Instituto de Medicina Molecular Joao Lobo Antunes (iMM)

This document may not be copied, reproduced, or modified in whole or in part for any purpose without written permission from the MAGIC Consortium. In addition to such written permission to copy, reproduce, or modify this document in whole or part, an acknowledgement of the authors of the document and all applicable portions of the copyright notice must be clearly referenced. All rights reserved.

## Disclaimer

The content of this deliverable does not reflect the official opinion of the European Union. Responsibility for the information and views expressed herein lies entirely with the author(s).

## History

Version	Date	Description	Reviewer
V0.1	10/05/2024	BIOND draft for internal review	FST & SD
V0.2	23/05/2024	KCL draft for internal review	FST
V0.3	31/05/2024	Addition of UCL and KCL sections to V0.1	AS, NG
V1.0	04/06/2024 05/06/2024	Final version approved Submission to EU	CR

## Author(s) list

Organisation	Name Surname	Email
UCL	Francesco Saverio TEDESCO (FST)	f.s.tedesco@ucl.ac.uk
UCL	Sumitava DASTIDAR (SD)	s.dastidar@ucl.ac.uk
BIOND	Nikolas GAIO (NG)	nikolas@biondteam.com
BIOND	Mitchell HAN (MH)	m.han@biondteam.com
KCL	Andrea SERIO (AS)	andrea.serio@kcl.ac.uk

## Table of Contents

Copyright.....	2
Disclaimer.....	2
History.....	3
Author(s) list.....	3
Table of Contents.....	4
List of Tables.....	5
List of Figures.....	5
Abbreviations and Acronyms.....	6
Executive Summary.....	7
1. Materials and Methods.....	8
2. Summary of activities and research findings.....	12
2.1 Generation of 3D engineered muscles from multiple muscle disorders (UCL, KCL).....	12
2.1.1 Duchenne Muscular Dystrophy (DMD).....	12
2.1.2 X-Linked Myotubular Myopathy (XLMTM).....	13
2.1.3 <i>LMNA</i> -related congenital muscular dystrophy (L-CMD).....	15
2.1.4 Ullrich Congenital Muscular Dystrophy (UCMD).....	17
2.2 3D artificial muscles generated with the MUSbit™ platform.....	19
2.2.1 Optimization of tissue formation.....	19
2.2.2 Tissue morphology and differentiation.....	20
2.2.3 Protocol transfer to UCL.....	21
3. Conclusions.....	23
References.....	23

## List of Tables

Table Nr	Title	Page Nr
Table 1	Detailed layout of 3D multi-lineage muscles generated for different diseases and different cell types used in the generation	9
Table 2	Details of the established protocols used to differentiate iPSCs to different cell types for the various diseases.	9

## List of Figures

Figure No.	Title	Page Nr
Figure 1	DMD bi-lineage skeletal muscle derived from patient iPSCs derived myogenic cells and patient fibroblasts.	13
Figure 2	DMD Trilineage skeletal muscle derived from patient iPSCs derived myogenic, endothelial and neuronal cells.	14
Figure 3	XLMTM 3D artificial bi-lineage skeletal muscle consisting of myogenic cells and patient fibroblasts.	15
Figure 4	XLMTM 3D artificial bi-lineage skeletal muscle consisting of myogenic and neuronal cells derived from patients hiPSCs.	16
Figure 5	LMNA 302P 3D artificial bi-lineage skeletal muscle derived from patients iPSCs derived myogenic cells and patient fibroblasts.	17
Figure 6	LMNA 3D artificial consisting of myogenic and neuronal cells derived from patients hiPSCs.	18
Figure 7	Immunofluorescence analysis of the Isogenic 3D myo-EM models for UCMD.	19
Figure 8	ioSkeletal Myocytes™ Engineered Microtissue formation and yield in MUSbit™	21
Figure 9	ioSkeletal Myocytes™ 3D Engineered Microtissues show tissue maturation	22
Figure 10	Generation of 3D muscles on MUSbit™ chip.	23

## Abbreviations and Acronyms

Acronym	Description
MAGIC	Next-Generation Models and Genetic Therapies for Rare Neuromuscular Diseases
WP	Work-Package
D	Deliverable
iPSC	Induced pluripotent stem cells
HIDEMs	Human iPSC-derived mesoangioblast-like inducible myogenic cells
PDMS	Polydimethylsiloxane
DMD	Duchenne muscular dystrophy
L-CMD	LMNA-related congenital muscular dystrophy
UCMD	Ullrich congenital muscular dystrophy
XLCNM/XLMTM	X-linked centronuclear myopathy / X-linked myotubular myopathy
GFP	Green Fluorescence Protein
MTM1	Myotubularin
<i>COL6A1</i>	Collagen type VI alpha 1 chain
LMNA	Lamin A/C
ECM	Extracellular Matrix
BSA	Bovine Serum Albumin
HUVECs	Human Umbilical Vein Endothelial Cells

## Executive Summary

Muscular dystrophy and other neuromuscular diseases are one of the major causes of disability worldwide that causes muscle wasting and weakness. While there is no effective cure, gene therapy has shown promise in treating other diseases and is being explored as a potential treatment for multiple neuromuscular diseases and dystrophies. While there has been significant progress in field, but there still exists major bottlenecks. One of which is nonavailability of humanized complex disease models, which is predictive, cost effective, mutation specific and rapid in development, in which the therapeutics can be assessed and refined. Hence, our overarching goal is to establish new advanced quasi-vivo models of human muscle disorders which will be used for the development of novel therapeutics strategies and vectors.

Under WP1, we are building new robust in vitro models of human muscle and neuromuscular disorders. In D1.1, UCL optimised and successfully generated multilineage 3D muscle models using available PDMS scaffolds. Myogenic, vascular, neural and fibrogenic cells were co-cultured in different combinations relevant to the target diseases of our project, namely DMD, L-CMD, UCMD and XLCNM. KCL contributed to the generation of motor neurons, whilst performing groundwork on microfabricated devices for D1.2. BIOND also validated their scaffold producing 3D muscles, which were also tested by UCL. Specifically, BIOND performed work using Duchenne Muscular Dystrophy (DMD) cells in the MUSbit™ device. Starting from a previously developed model, BIOND replaced wild type cells with DMD cells and refined protocols to suit this adaptation. Subsequently, they monitored the formation of the engineered tissues and characterized their morphology through immunofluorescent staining using a muscle differentiation marker.

## 1. Materials and Methods

**Scaffolds:** The 3D muscles were generated using existing validated PDMS scaffolds from EHT technologies (now Dinabios) [1].

### Cells

Myogenic cells, motor neurons, endothelial cells and fibrogenic cells were differentiated from human iPSCs (hiPSCs) using protocols previously described by UCL in [2]. For neuronal differentiation of XLCNM iPSCs, an additional transgene-based protocol was used, details of which are described in [3]. Alternatively, human adult tissue-derived cells such as immortalised myoblasts, dermal fibroblasts or human umbilical vascular endothelial cells (HUVECs) were used, detailed in **Table-1**. Fibroblasts for all the disease types were labelled with a lentiviral vector expressing a constitutive GFP reporter transgene to facilitate detection. Culturing and maintenance of the all-cell types were performed as described in [2, 3].

BIOND's tissues were obtained utilizing bit.bio's Opti-ox™ cells. While human induced pluripotent stem cells (hiPSCs) present a promising foundation for skeletal muscle cell derivation, their widespread application has been impeded by the challenges associated with complex and inconsistent differentiation protocols. Opti-ox™ cells are designed to facilitate precise control over the expression of transcription factors. This advancement enhances the reprogramming efficiency of hiPSCs, streamlining the differentiation process. Here we use their ioSkeletal Myocytes™, specifically developed for rapid myogenic differentiation. Wild-type ioSkeletal Myocytes™ have previously been used in combination with the MUSbit™ chip for the development of healthy skeletal muscle models. Building upon this groundwork, our endeavor expands the utility of this cellular source by incorporating ioSkeletal Myocytes DMD Exon 52 Deletion™ and ioSkeletal Myocytes DMD Exon 44 Deletion™ variants.

### **Generation and characterisation of multi-lineage 3D muscles using PDMS scaffold:**

**Tri-lineage muscles:** For the tri-lineage muscles, the myogenic, neuronal and endothelial cells (totalling 1 million cells/ muscle) were mixed in a ratio of 8:1:1 during casting of the muscles. Post muscles casting for 48hrs the 3D muscles were maintained in proliferation condition before induction of differentiation. Termination of differentiation for the trilineage 3D muscles is cell line dependent, which ranges from day-5 to day-14 of differentiation. Detailed protocol for the trilineage muscles generated is described in our previous work [2]. Additionally, we also take modular approach, where neuronal cells can be layered on 3D muscles containing muscles and endothelial cells.

**Bi-lineage muscles:** Bi-lineage 3D myo-ECM model contains myogenic cells and fibroblasts. The bi-lineage set up was obtained with new proprietary protocol based on a mixture of both cell types. Bi-lineage 3D muscles were cultured under proliferation condition for 48h after which they were transferred into differentiation culture condition. Termination of differentiation was cell line dependent, which ranges from day-5 to day-7 of differentiation.

3D muscles were fixed with 4% paraformaldehyde (PFA) for 3 hr at 4°C followed by 6 hr of blocking at 4°C (10% FBS, 1% BSA, and 0.5% Triton X-100 in 0.05 M Tris-buffered saline [TBS]) before immunolabeling with primary antibody overnight at 4°C in TBS, 1% BSA, and 0.5% Triton X-100. On day two, muscles were washed with TBS 6 times hourly and incubated overnight with DAPI plus species-specific secondary antibodies. The following day, hydrogels were washed 6 times with TBS

and embedded in mounting medium and proceeded for confocal microscope for imaging. The images were analysed with Fiji software.

Disease	Multilineage type	Cell types included	Genotype
DMD	Bi-lineage muscles	iPSCs derived myogenic cells	<i>DMD</i> Ex68 (c.9851 G>A)
		Fibroblasts	<i>DMD</i> Ex68 (c.9851 G>A)
	Tri-lineage muscles	iPSCs derived myogenic cells, neuronal cells and endothelial cells	<i>DMD</i> Ex52-Del
		Isogenic WT-iPSCs derived myogenic cells, neuronal cells and endothelial cells	WT (isogenic control)
XLCNM (XLMTM)	Bi-lineage muscles	Immortalised myoblasts	<i>MTM1</i> Ex8 (c.594 C>G)
		Fibroblasts	<i>MTM1</i> Ex8 (c.594 C>G)
	Bi-lineage muscles	Immortalised myoblasts	WT
		Fibroblasts	WT
	Tri-lineage muscles	iPSCs derived myogenic cells, neuronal cells and endothelial cells	<i>MTM1</i> Ex8 (c.594 C>G)
		Isogenic WT-iPSCs myogenic cells, neuronal cells and endothelial cells	WT-isogenic
UCMD	Bi-lineage muscles	iPSCs derived myogenic cells	<i>COL6A1</i> (NM_001848 c.930+189 C>T)
		Fibroblasts	<i>COL6A1</i> (NM_001848 c.930+189 C>T)
	Bi-lineage muscles	iPSCs derived myogenic cells	WT
		Fibroblasts	WT
L-CMD	Bi-lineage muscles	Patient iPSCs derived myogenic cells	<i>LMNA</i> Ex5 (c.905 T>C)
		Fibroblasts	<i>LMNA</i> Ex5 (c.905 T>C)
	Tri-lineage muscles	iPSCs derived Myogenic cells, Neuronal cells and Endothelial cells	<i>LMNA</i> Ex5 (c.905 T>C)

**Table 1.** Cell types used in the generation of 3D muscles by UCL

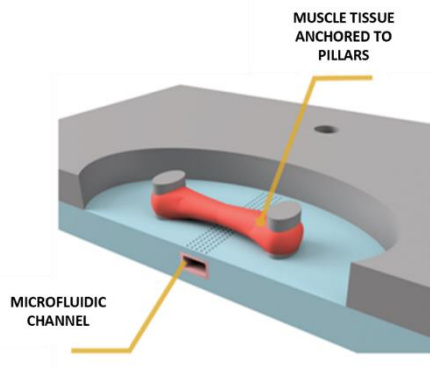
Differentiated cell	Source iPSCs	Differentiation Protocol
Myogenic cells	L-CMD, UCMD, XLCNM and DMD	Maffioletti, S. M. et al. 2018; Caron, L. et al. 2016, [1, 4]
Endothelial cells	L-CMD, XLCNM and DMD	Orlova, V. V. et al. 2014 [5]
Neuronal cells	L-CMD and DMD	Hall, C. E. et al. 2017 [6]
Neuronal cells	XLCNM	Fernandopulle, M.S. et al. 2018 [3]

**Table 2.** Details of the established protocols used to differentiate iPSCs to different cell types for the various diseases

### MUSbit™ Chip

To develop a new DMD model, BIOND utilised a hardware set comprising the MUSbit™ chips, used in combination with the SUP interface. Additionally, commercially available induced pluripotent stem cells (iPSCs) sourced from bit.bio were employed as the cellular foundation for our experiments. The MUSbit™ is a silicon-based microfluidic chip including micro-pillars that allow for the precise control and induction of skeletal muscle organoid formation. This feature is crucial for the accurate replication of the complex and dynamic nature of muscle tissue. Secondly, the device incorporates microfluidic channels, which enable the dynamic application of drugs within the model. This feature also allows for the performance of physiologically relevant absorption studies that can provide valuable insights into drug efficacy and side effects. These silicon based chips are scalable and have the potential to integrate multiple features according to customer needs. For instance, the chips allows multiple co-cultures, muscle microenvironments with specific cells, vascularization, chronic stimulation over hours/days, contraction forces, and compatible with a diverse range of imaging techniques and conventional assays. This deliverable focuses on DMD tissue formation around the pillars, using chips without microchannels. Deliverable 1.2 will transition the model to chips with channels.

During the first 6 months of the project, the MUSbit™ design was upgraded, following input and suggestions from BIOND early adopters.



Rendering of the MUSbit™ chip

SUP interface. MUSbit™ chips are provided in a single-use plate (SUP) interface (Figure 2), featuring a multi-well format. Each plate accommodates 12 centrally positioned MUSbit™ chips, surrounded by smaller wells for PBS filling to prevent evaporation. Currently, BIOND is in the process of developing higher throughput SUPs.

This housing design allows for concurrent testing of multiple samples, enhancing efficiency and user-friendliness. It seamlessly integrates with standard biological laboratory practices, including microscopy, sampling, and culturing procedures. During the first 6 months of the project, the SUP designed was upgraded, following input and suggestions from BIOND early adopters.



Picture of the SUP interface, equipped with 24 MUSbit™ chips



Chip preparation. The current version of the MUSbit™ chip surface exhibits hydrophobic properties, requiring performing a treatment before pipetting small volumes of hydrogel/cell mixture into the chip. To obtain a uniform seeding in the chip well, we recommend performing a plasma treatment of the SUP (including the MUSbit™ chips) to render the chip hydrophilic. The following plasma conditions are suggested: initial pressure of 0.15 mbar followed by pure O<sub>2</sub> injection. After that the chip should be exposed to a pulsating pressure of 0.2-0.25 mbar, input power of 20 W, for 180 seconds.

The SUP is then sterilized in a biosafety cabinet. The hardware is sprayed and wiped with 70% ethanol or IPA. The chip wells are then filled with 250 µL of 70% IPA/ethanol and the outer wells with approximately 150 µL of the same solution, then incubated for 10 minutes. The IPA/ethanol solution is then aspirated from the chip wells, avoiding entry into the chip well to prevent damage to the PDMS or pillars. The wells are then washed twice with 200 µL of dPBS.

Cell seeding. Before injecting the cells in the wells, they are embedded in a hydrogel. After the hydrogel/cell mixture is pipetted into the chips and fully gelled, medium is added. The cell/gel suspension self-compact around the pillars over the course of the next hours/days, resulting in the formation of a skeletal muscle bundle. We routinely seed 12-24 chips per experiment per cell line. The optimal cell density needs to be optimized empirically for each cell type. For ioSkeletal Myocytes DMD Exon 52 Deletion™ and ioSkeletal Myocytes DMD Exon 44 Deletion™ we identified an optimal working cell density of 30,000 cells per microtissue (15 million cells/ml). 2D controls were seeded at a 125,000 cells/cm<sup>2</sup> in a Ibidi 18-well µslide (Cat No. 81816) coated with Geltrex™ LDEV-Free Reduced Growth Factor Basement Membrane Matrix (Thermo Fisher). 24 hours after seeding, the well medium is replaced with differentiation Medium + 2 mg/ml ACA. For the first few days, a partial medium exchange is preferred to avoid bundle detachment. When a clear bundle construct is formed, full volume media changes were performed every 2-3 days.

Model characterization. To monitor bundle formation, images of chips were recorded on days every other day. Success was assessed as tissues attached between the two MUSbit™ pillars. The morphology and differentiation state of the cells were assessed at Day 5 and Day 9 after seeding using Whole-mount Immunofluorescent Staining. In short, tissues were stained for Sarcomeric Alpha Actinin (Clone EA53 – Sigma Aldrich) to assess myofiber striation or Dystrophin (Clone MANDYS106 – Sigma Aldrich) as control for the DMD cell lines, and counterstained with Phalloidin for Actin and DAPI for the nuclei. Tissues were imaged on a Nikon Ti-eclipse coupled with a Crest X-light V3 Spinning Disk confocal unit. Data is represented as maximum intensity projections. Samples were imaged using the exact same microscope capture settings, and their LUT ranges were set the same across the different conditions, to allow a fair comparison of fluorescence intensity.

## 2. Summary of activities and research findings

### 2.1 Generation of 3D engineered muscles from multiple muscle disorders (UCL, KCL)

UCL has focused efforts to expand and optimise the procedure to generate multilineage 3D muscle models using readily available PDMS scaffolds for multiple target diseases, namely DMD, L-CMD, UCMD and XLCNM.

#### 2.1.1 Duchenne Muscular Dystrophy (DMD)

In the case of DMD, we first generated multi-lineage constructs containing myotubes/myofibres and fibrogenic cells (i.e. fibroblasts or FAPs: fibroadipogenic progenitors). We generated myogenic cells from a DMD hiPSC line carrying a pathogenic mutation Exon 68 (c.9851 G>A). Myogenic cells were combined with GFP-expressing fibroblast derived from the same patient to obtain the bi-lineage muscles (Figure 1A). Hydrogels with only fibroblasts or myoblasts were taken as control conditions. We could obtain polymerized gels containing the cells. As in Figure 1A, day 3 microscopic analysis showed presence of GFP positive fibroblasts (only myoblasts gel- neg control) as seen under a stereomicroscope. Upon immunofluorescence staining, we could detect MyHC positive mature myotube and GFP positive fibroblasts in the 3D muscles. The myogenic differentiation in the bi-lineage muscles was similar to only myoblasts condition, indicating no hindrance of fibroblasts on muscle formation.

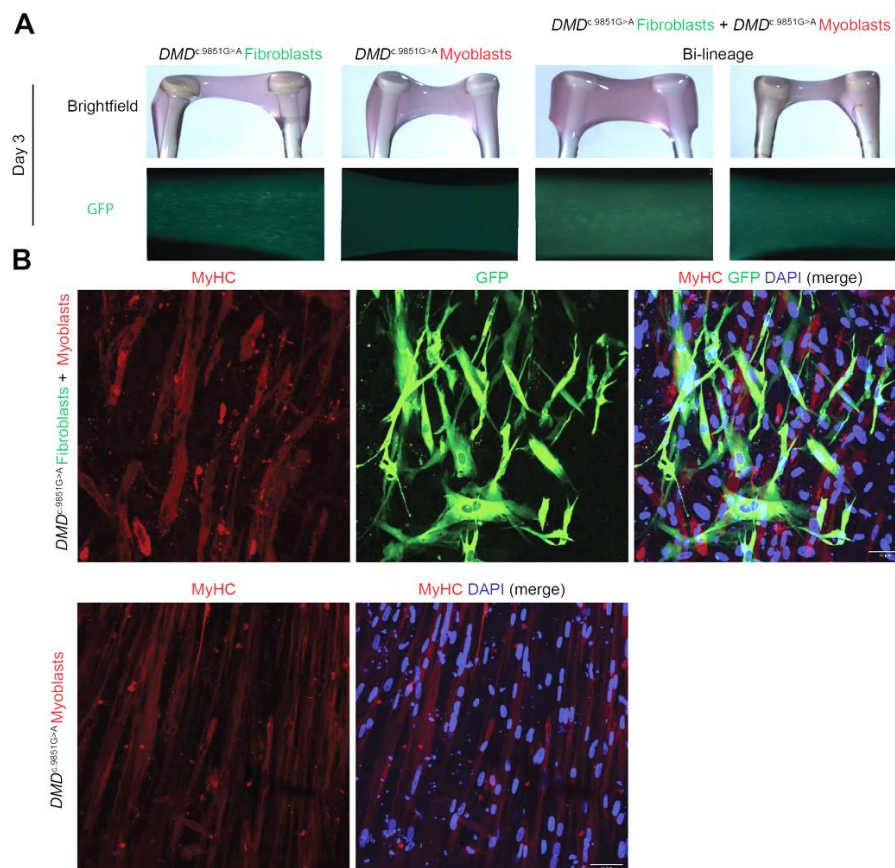


**Figure 1.** *DMDc.9851G>A* 3D bi-lineage (isogenic) skeletal muscle from patient iPSC-derived myogenic cells and patient fibroblasts. **(A)** Stereoscopic images of the engineered muscles containing iPSC derived myoblast and GFP labelled fibroblasts imaged at day 3 of differentiation. **(B)** Immunofluorescence images of *DMDc.9851G>A* Fibroblasts + *DMDc.9851G>A* Myoblasts and only *DMDc.9851G>A*. Nuclei were stained with DAPI. Scale bar 50  $\mu$ m. MyHC: myosin heavy chain, GFP: green fluorescence protein. (ABMyHC, redGFP, greenblue)

Having successfully generated bi-lineage muscles, we moved to increase the complexity of the DMD muscles by incorporating endothelial (ECs) and motor neurons (MNs) with iPSC-derived myogenic cells. We used a new DMD iPSC line with its matched isogenic control which has been engineered with a reporter transgene (Rep) to be used in subsequent work packages. Its noteworthy to mention that as a positive control for iPSCs derived endothelial, we had generated muscles with HUVECs instead of ECs. Figure 2A depicts 3D muscles obtained under different conditions. Immunofluorescence analysis of 3D muscles showed MyHC positive myotubes and myocytes Figure 2B. We could detect presence of CD31+ ECs in the muscles like in the control condition where we had incorporated HUVECs (the latter colonising muscle more efficiently than iPSC derived ECs). Expectedly the overall frequency of ECs was low compared to myogenic cells as the input ratio of ECs to myogenic cells was 1:10 (Figure 2B). In addition to ECs, we also stained the 3D muscles for presence of SMI32+ motor neurons (MNs). As shown in Figure 2B, we could detect presence of SMI32+ MNs in small clusters between the MYHC+ myofibers/myocytes.

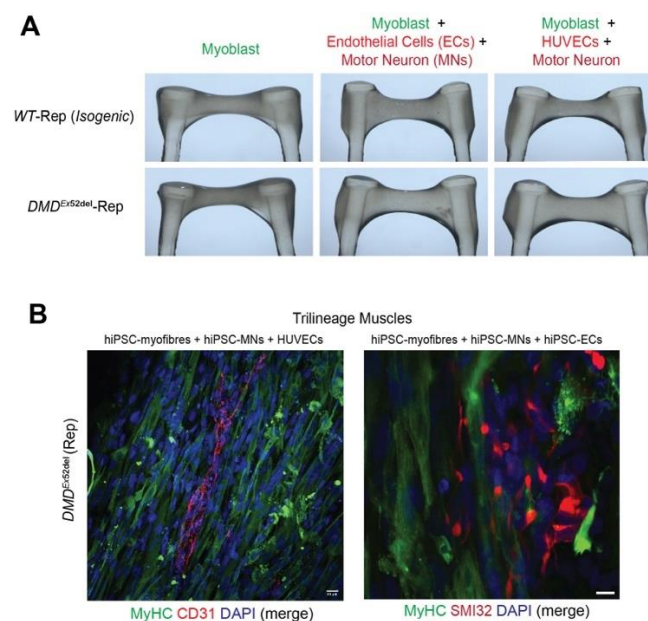


**Figure 2.** DMD and WT trilineage 3D skeletal muscles. (A) Stereomicroscope images of the 3D artificial skeletal muscles containing iPSC derived myoblast, endothelial cells and motor neurons captured on day 3 of differentiation. (B) Representative immunofluorescence images of DMD 3D tri-lineage muscles made with hiPSC-derived myofibres (MyHC), MNs (SMI) and ECs (left) or HUVECs (right image). CD31 identifies HUVECs or hiPSC-derived ECs. Nuclei were stained with DAPI (blue).

### 2.1.2 X-Linked Myotubular Myopathy (XLMTM)

For X-linked centronuclear/myotubular myopathy (XLCNM/XLMTM), we aimed to generate multilineage 3D muscles for the first time. We first verified if XLMTM hiPSC-derived muscles cells could differentiate in the hydrogels if combined with muscle fibroblasts. Hence, primary healthy muscle fibroblasts were combined with healthy control (control) or with CRISPR-Cas9 corrected hiPSC-derived myoblasts (isogenic control) and the XLMTM patient fibroblasts were combined with XLMTM hiPSC-derived myoblasts (XLMTM) (Figure 3). Immunofluorescence images of the bi-lineage gels show co-existence of GFP+ fibroblasts with myosin heavy chain (MyHC)+ myotubes which aligned along the main axis of the 3D muscle constructs (Figure 3A-B).

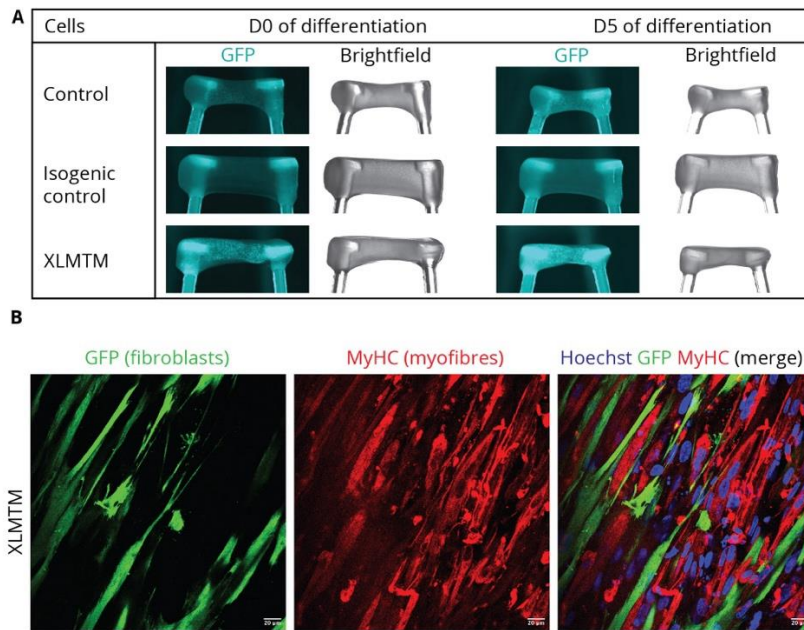


**Figure 3.** XLMTM 3D artificial bi-lineage skeletal muscle consisting of myogenic cells and patient fibroblasts. (A) Stereoscopic images of 3D artificial muscles containing GFP labelled primary fibroblasts and iPSC derived myoblasts on day 0 and day 5 of differentiation. Hydrogels were cast containing primary healthy fibroblasts with healthy control iPSC derived myoblasts (control), XLMTM patient fibroblasts and XLMTM iPSC derived myoblasts and respective isogenic controls. (B) Immunofluorescence images of XLMTM bi-lineage engineered muscles containing GFP+ fibroblasts (GFP) and myofibers (MyHC). Nuclei were stained with Hoechst. Scale bar 20  $\mu$ m. MyHC= Myosin Heavy Chain

Having confirmed that the XLMTM muscle cells can differentiate into myotubes when combined with different cell types, we generated isogenic control and XLMTM hiPSC-derived MNs and ECs (Figure 4A-B). hiPSC-derived motor neurons were obtained using a transgene-based protocol. hiPSCs were transfected with hNIL construct to overexpress neurogenin 2, ISL-1 and LHX-3 under a doxycycline inducible promoter in close collaboration with KCL (Dr. Taylor Minckley, Serio lab). The hNIL plasmid was stably integrated into the cells with co-transfection of hyperactive piggyBac transposon. We selected the hiPSCs with transgene insertion thanks to the stable expression of nuclear-localised BFP (by flow cytometry) and resistance to puromycin. We then combined the isogenic control and XLMTM hiPSC-derived MNs with the respective hiPSC-derived muscle cells in the hydrogels. After 5 days in differentiation media, we obtained isogenic SMI32+ MNs and MyHC+ multinucleated myotubes co-existing in the same 3D muscle constructs (Figure 3).

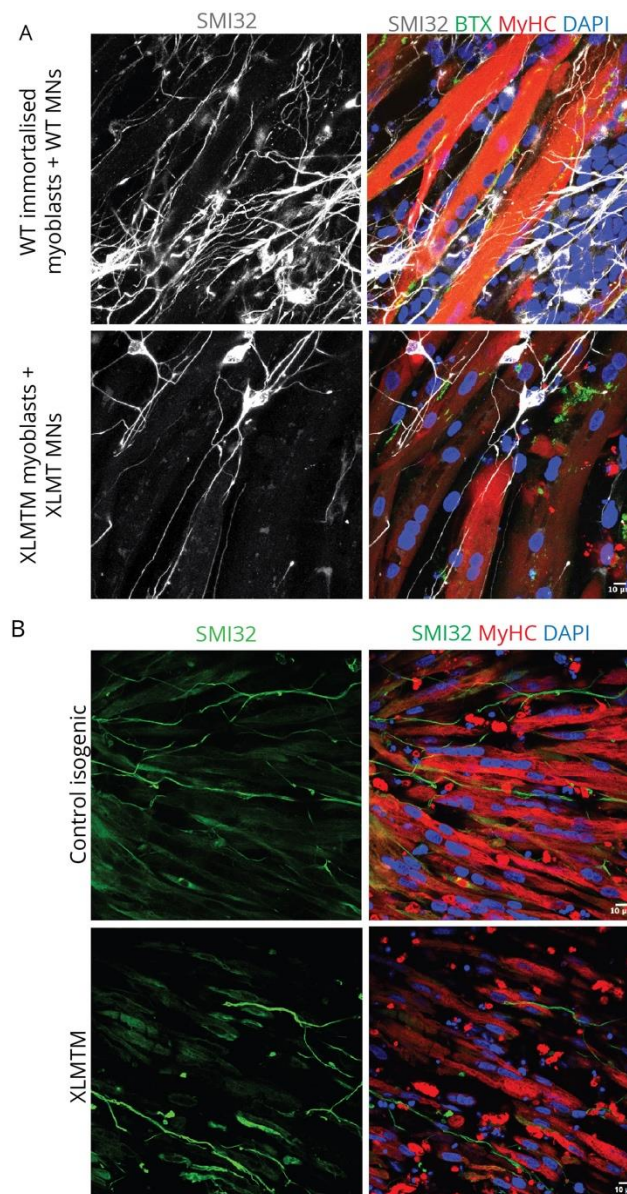


**Figure 4.** XLMTM 3D artificial bi-lineage skeletal muscles containing MNs. (A) Confocal images of 15 day post-differentiation XLMTM bilineage construct containing healthy (WT) control and XLMTM immortalised muscles (MyHC, red) combined with hiPSC-derived transgene-based SMI32+ MNs (white) and showing alpha-bungarotoxin (BTX)+ acetylcholine receptors (green). Nuclei are stained with DAPI. Scale bar 10  $\mu\text{m}$ . (B) Confocal images of 5 day post-differentiation XLMTM bi-lineage constructs containing hiPSC-derived transgene based SMI32+ (green) and hiPSC-derived myofibers (MyHC, red). Nuclei are stained with DAPI. Scale bar 10  $\mu\text{m}$

### 2.1.3 LMNA-related congenital muscular dystrophy (L-CMD)

For L-CMD we have increased the complexity of 3D engineered disease models by including supporting cell types such as fibroblasts and motor neurons in an isogenic manner. Those two supporting cell types have been selected in view of their potential relevance in terms of pathogenesis, as fibrosis and contractures are a prominent feature of L-CMD and mutation in LMNA also cause a peripheral neuropathy. Combination of iPSC-derived myoblasts and GFP-labelled fibroblasts from the same patient carrying the L-CMD-causing *LMNA* L302P mutation generated bi-lineage engineered muscles (Figure 5). These muscles recapitulated hallmark nuclear shape abnormalities of laminopathies, using a transgene-free protocol for myogenic differentiation which enables examination of early myogenic differentiation phenotypes. Further

analysis of these muscles may enable us to examine interactions between extracellular matrix and myofibres as to study the severe fibrosis which is well documented in this condition.

Secondly, bi-lineage engineered muscles combining differentiated muscle cells and MNs were made using iPSC-derived cells from the *LMNA* L302P hiPSC line (Figure 6). Combining the three cell types demonstrated successful differentiation of all three cell lineages within the engineered muscle through immunolabelling of myosin heavy chain (muscle) and SMI32 (MNs). This demonstrates the ability of our system to support multilineage modelling of laminopathy muscle tissues. This work will enable cell-type specific examination of laminopathy disease phenotypes in an isogenic manner, enabling tissue- and cell-specific modelling in future experiments.

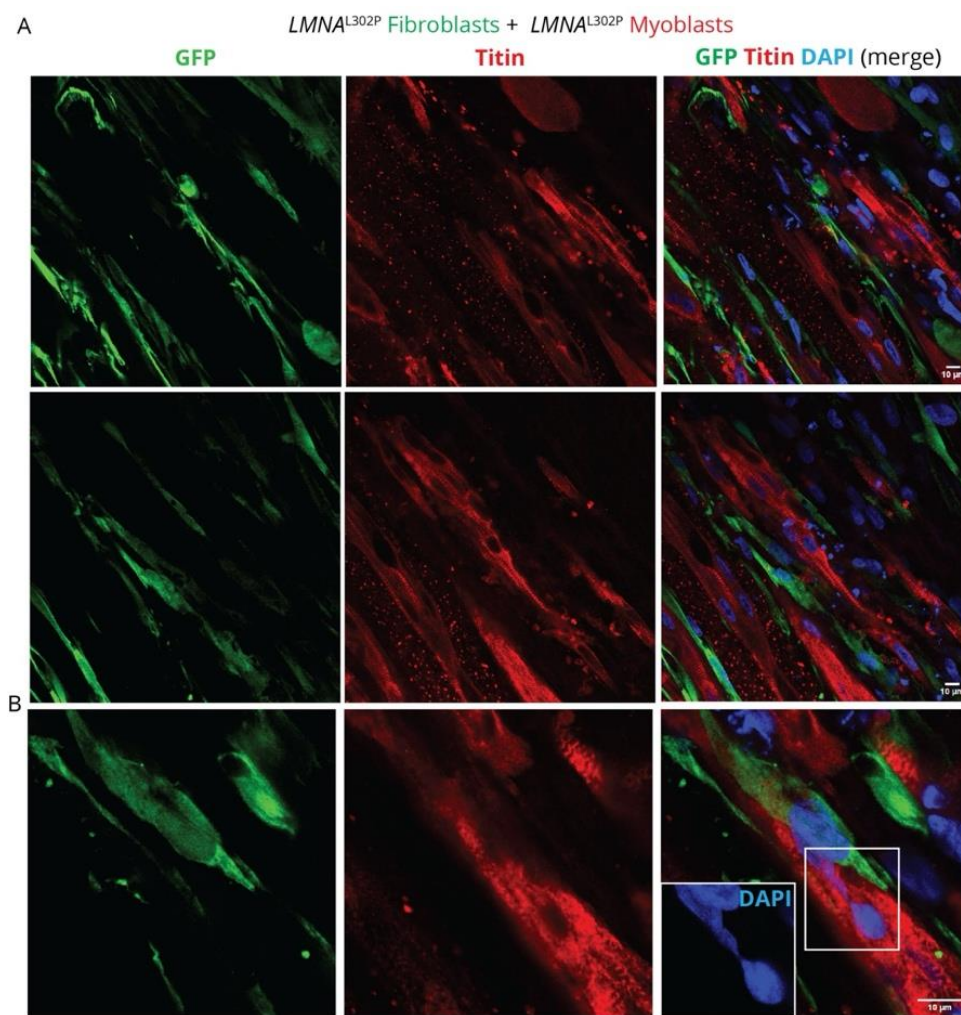


Figure 5: *LMNA*<sup>L302P</sup> 3D artificial bilineage skeletal muscle derived from patients iPSCs derived myogenic cells and patient fibroblasts. (A) Confocal images of *LMNA*<sup>L302P</sup> bilineage construct containing GFP+ fibroblasts (GFP, green) and myofibers (titin, red). Nuclei are stained with DAPI. Scale bar 10 μm. (B) Zoomed confocal image of *LMNA*<sup>L302P</sup> bilineage constructs showing abnormal myonuclei stained with DAPI (blue).

Figure 5

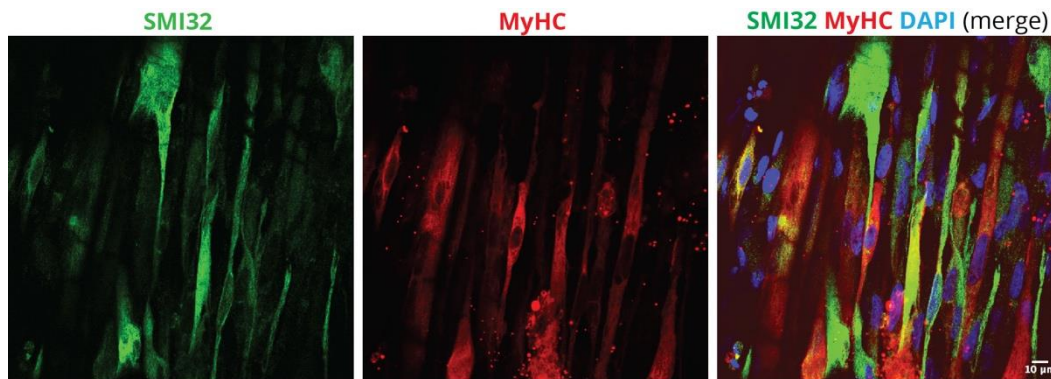
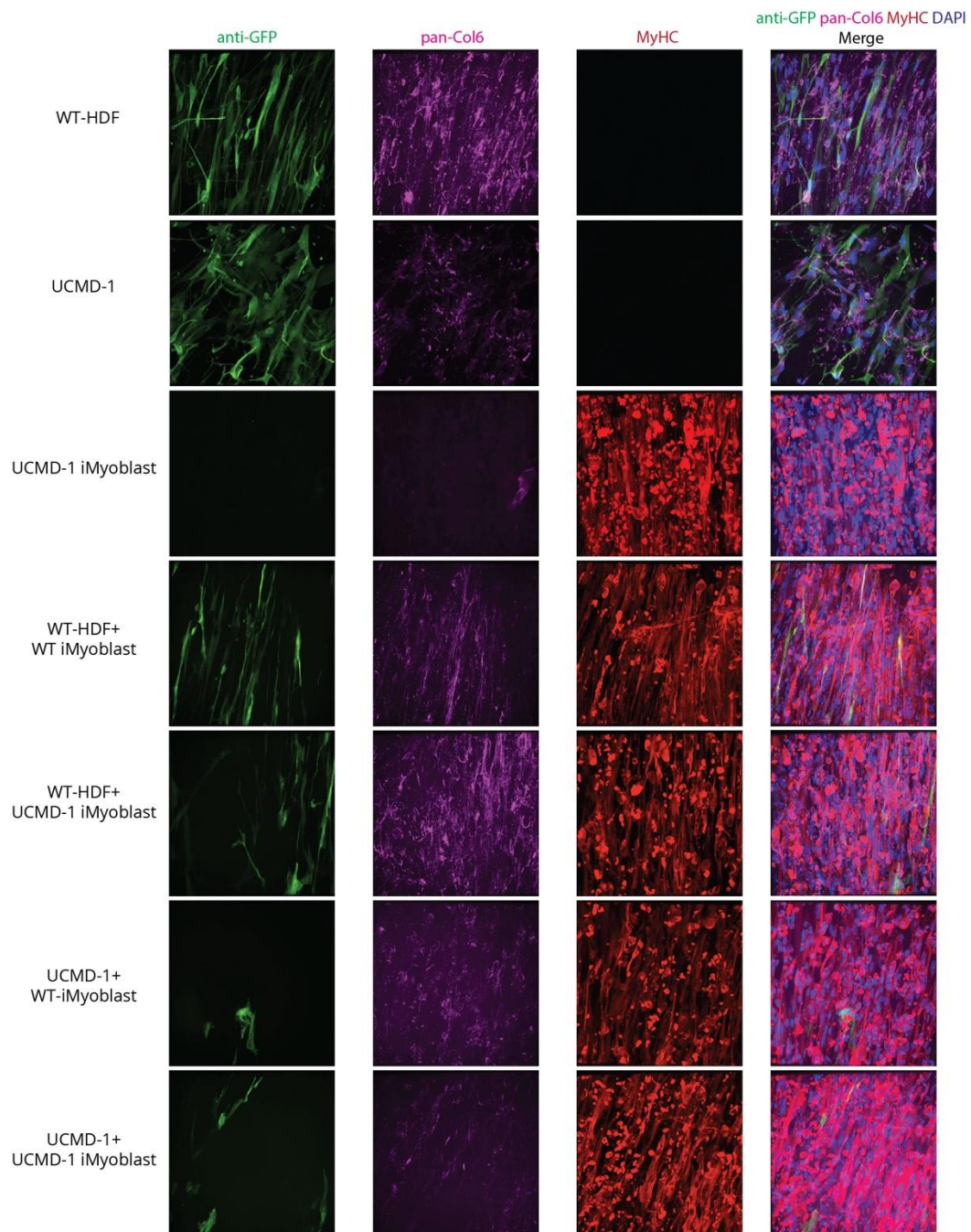


Figure 6: *LMNA*<sup>L302P</sup> 3D artificial bilineage muscle derived from patients iPSC. Confocal images of *LMNA*<sup>L302P</sup> bilineage construct containing motor neurons (SMI32, green) and myofibers (MyHC, red). Nuclei are stained with DAPI (blue). Scale bar 10  $\mu$ m.

Figure 6

### 2.1.4 Ullrich Congenital Muscular Dystrophy (UCMD)

To model UCMD the Tedesco lab at UCL have established a new model that encapsulates both ECM-depositing fibroblasts and myotubes derived from tissue-derived myoblasts with the aim to uncover novel pathogenic hallmarks and clinically relevant phenotypic readouts of Col6-RDs *in vitro*. Such model enables us to recapitulate disease associated phenotypes of UCMD patients including the hallmark contracture phenotype. Here, we further advanced this model by incorporating human induced pluripotent stem cell (hiPSCs)-derived myoblasts into the 3D myo-ECM model. hiPSCs-derived myoblasts were generated using a transgene-free protocol that allows recapitulation of developmental myogenesis and may further enable identification of under-recognized or undetermined early pathogenic phenotypes during development once incorporated into the 3D myo-ECM model. We constructed 3D myo-ECM models of WT human dermal fibroblasts (WT-HDF) or UCMD patient-derived skin fibroblasts (UCMD-1) cocultured with myoblasts generated from either WT hiPSC (WT iMyoblast) or from a new UCMD-1 patient-derived hiPSC line (UCMD-1 iMyoblast). The fibroblast line was transduced with GFP-expressing lentiviral vectors to distinguish them from myogenic cells upon co-culture. After performing immunostaining on fixed samples, we observed deposition of Collagen VI matrix in both WT-HDF and UCMD-1 models but not in the model with only UCMD-1 iMyoblasts as expected. Furthermore, in the coculture 3D models, Col6 proteins deposited by GFP-positive fibroblasts showed close spatial interactions with myosin heavy chain-positive myotubes derived from the iMyoblasts (Figure 7), further validating the myotube-matrix interactions in a 3D environment created in these myo-ECM models.



**Figure 7.** Whole-mount immunofluorescence for anti-GFP (green), pan-Col6 protein (magenta) and myosin heavy chain (MyHC; red) in fibroblast-only (WT-HDF or UCMD-1), UCMD-1 iPSC derived myoblast-only (UCMD-1 iMyoblast) and 3D myo-ECM cultures with both iPSC-derived myoblasts (WT or UCMD-1 iMyoblasts) and fibroblasts (WT or UCMD-1). DAPI was used for nuclei staining. 3D hydrogel was differentiated for 4 days before fixation. Scale bar: 25 $\mu$ m.

## 2.2 3D artificial muscles generated with the MUSbit™ platform

### 2.2.1 Optimization of tissue formation

BIOND previously established a protocol to generate skeletal muscle microtissues into their MUSbit™ chip using ioSkeletal Myocytes™, wild-type human hiPSC-derived skeletal myocytes (Figure 8A - top row). In short, cell-laden hydrogels are seeded in the MUSbit™ chips. Over the course of days the gel compacts around the MUSbit™ pillars and eventually forms a contractile muscle bundle. Experience with other cell lines informed us that the cell seeding density has a big effect on bundle formation, and that this needs to be optimized for each cell line separately. Here we varied the cell density during cell seeding for the DMD variants of ioSkeletal Myocytes™: ioSkeletal Myocytes DMD Exon 44 Deletion™ (DMD Del44) and ioSkeletal Myocytes DMD Exon 52 Deletion™ (DMD Del52).

There is a clear effect of cell density in the yield of bundle formation of these cell lines from Day 7 onwards (Figure 8B), with a seemingly optimal seeding density of 35,000 cells/gel for DMD Del44, while DMD Del52 shows an optimum at 30,000 cells/gel. Interestingly, DMD Del44 seems to favor higher cell densities (35,000 cells/ml), while this density gives a lower yield for the DMD Del 52. Indeed, the progression of the morphology of the bundles is different for both DMD lines compared to wild-type (Figure 8A). DMD del44 bundles look markedly bulkier compared to wild-type, possibly pointing to proliferation of a part of the cell population. In contrast, DMD del 52 bundles are “skinnier” than wild-type bundles. This difference in response between the two DMD lines mimic the physiological DMD disease with several gene variants giving different patient and therapeutic outcomes.

As previous experiments with the wild-type variant were done with 30,000 cells/ml, all further experiments were done with this density with all cell lines. The yield of both DMD lines are comparable to wild-type up to at least Day 7, with both lines having even higher yields for these sets of experiments compared to wild-type (Figure 9C). While there is obvious room for improvement for longer-term studies, wild-type ioSkeletal myocyte bundles are already contractile from Day 7, and sufficient bundles per experiment survive for data collection. We therefore went ahead with our current protocol for downstream functional studies.

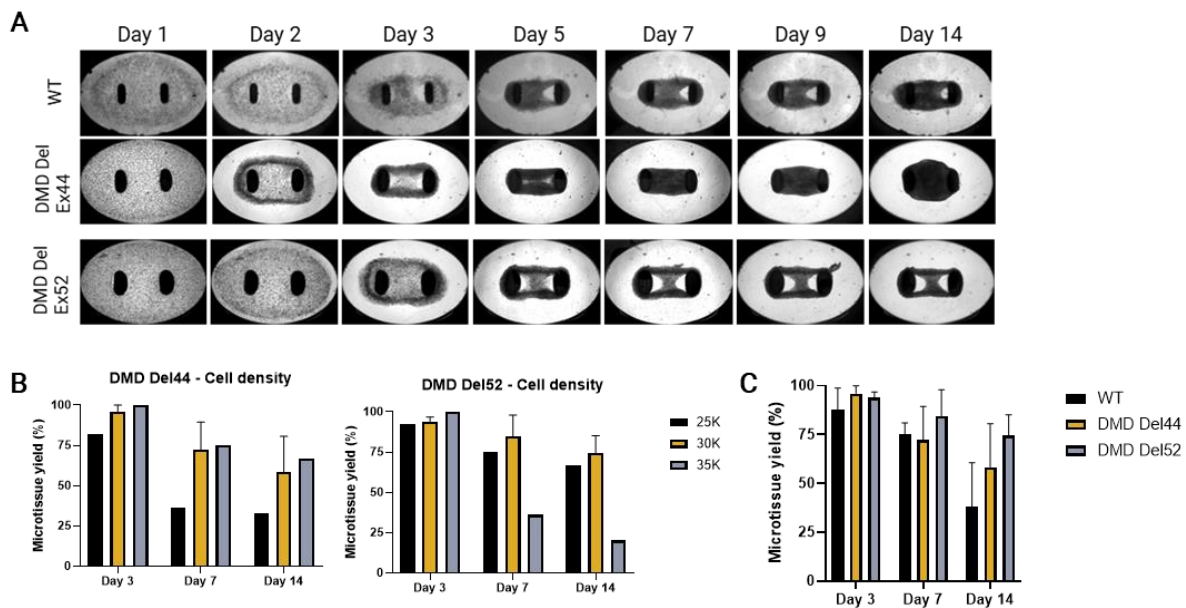


**Figure 8.** *ioSkeletal Myocytes™* Engineered Microtissue formation and yield in MUSbit™

## 2.2.2 Tissue morphology and differentiation

To further characterize the 3D engineered microtissues, we fixed the bundles at Day 9 after seeding and performed immunostaining. We stained bundles for Sarcomeric alpha-actinin (SAA) to identify differentiation and maturation of myotubes, as well as Dystrophin (Dys) as control for the DMD cell lines. Qualitatively we find that both DMD lines show similar differentiation compared to wild-type muscle bundles (Figure 9A and B). This indicates that the loss of DMD protein in these cells does not seem to inhibit their differentiation, similar to their 2D counterparts (<https://www.bit.bio/products/muscle-cells/skeletal-myocytes-dmd-exon-44-deletion-io1018>).

For all lines, SAA positive fibers seem to be enriched in the outer rim of the bundle. We postulate a higher amount of differentiation in this area of the tissue because of higher tension and/or a higher density of cells during compaction compared to the middle in-between the two pillars.

Upon closer inspection, we find similar tissue organization for wild-type and DMD Del44 (Figure 10B). DMD Del52 however, seems to be less dense and myofibers seem more apparent due to less cells in the tissue. Overall less nuclei are present and a higher proportion of fragmented nuclei (which we see in all lines) can be observed as the small dotted structures in the DAPI image. This correlates well with the observation that DMD Del52 show an overall skinnier morphology. For control we also stained bundles for Dystrophin (Figure 9 C and D). In wild-type tissues we find dystrophin uniformly expressed as expected, while DMD lines show markedly less signal. While there is likely non-specific staining of the hydrogel, as well as some antibody aggregates as evidence by the dotted structures in the higher magnification images (Figure 9D), we cannot fully rule out the total loss of dystrophin expression in these DMD lines. Indeed, qPCR suggests some residual DMD expression in these DMD deletion lines ([\[bit.bio website\]](https://www.bit.bio)), with DMD Del44 showing higher expression than DMD Del52. This would correlate with a slightly higher intensity of Dys staining in the DMD Del42 line compared to the DMD Del52.

In any case, the high proportion of SAA-positive fibers indicate that the DMD lines should be contractile, similar to what we have shown before for wild-type (<https://resources.gobiond.com/download-poster-skeletal-muscle>). Indeed, in preliminary experiments we find that they contract under electrical pulse stimulation (data not shown). Further experiments will clarify if there is a functional difference between the DMD lines and wild-type.

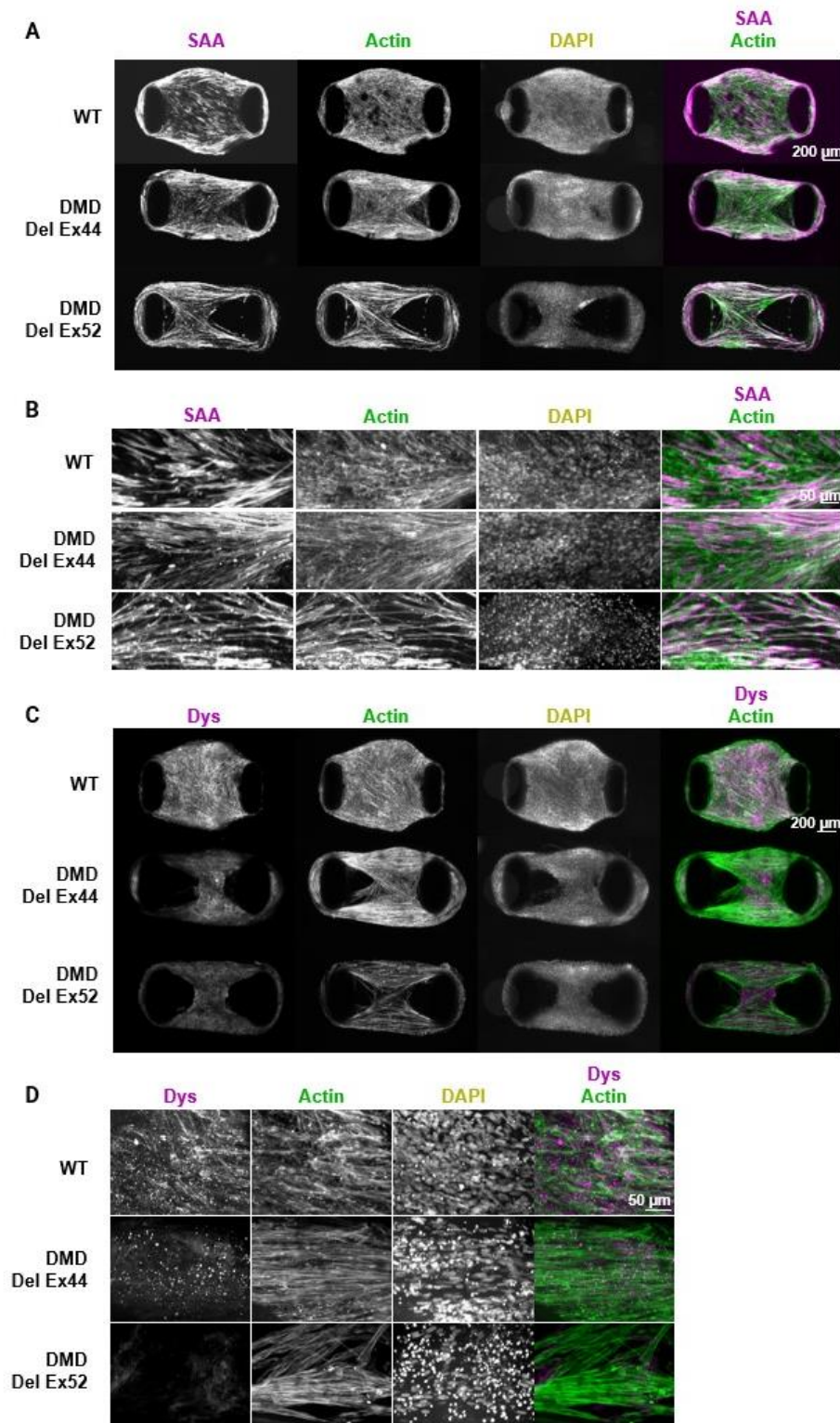


Figure 9. ioSkeletal Myocytes™ 3D Engineered Microtissues show tissue maturation

### 2.2.3 Protocol transfer to UCL

BIOND transferred the protocol to the Tedesco lab at UCL. During this first phase of the project 12 chips were tested with two different cell densities (20,000 cells/ muscle & 30,000 cells/muscle) of myogenic cells from healthy control line. Post day 5 of differentiation, the Myo bundles obtained

were analysed for myogenic markers. Presence of myofibers were detected which were positive for Myosin Heavy Chain (MyHC) and TITIN muscle markers (Figure 10A). We did not observe any significant difference in Myo bundle formation when compared between two cell densities. The presence of differentiated myofibres signifies the broad applicability of the previously developed protocol and successful transfer of the protocol to a MAGIC partner. Additional experiments were performed where we included two new cell lines in addition to the healthy control line. iPSCs derived myogenic cells of MTM patients along with its isogenic control was tested at high cell density of 30,000 cells/muscle. Compared to the control cell line, macroscopic tissue morphology and skeletal myogenic differentiation from the other cell lines was less uniform (Figure 11B). Further optimisation experiments are ongoing for subsequent deliverables.

Additional comments on the working protocol were given as feedback and will be actively worked on by BIOND to improve chip handling, cell seeding, and usage of BIOND products for downstream assays. The main challenge seems to be the handling of the gel mixture during seeding, where the short polymerization time could affect the amount of chips to be seeded simultaneously. We are thus currently investigating the sourcing of new materials (in more ready-to-use formats) and testing it with our current working protocol to reduce the challenges for the end-user.

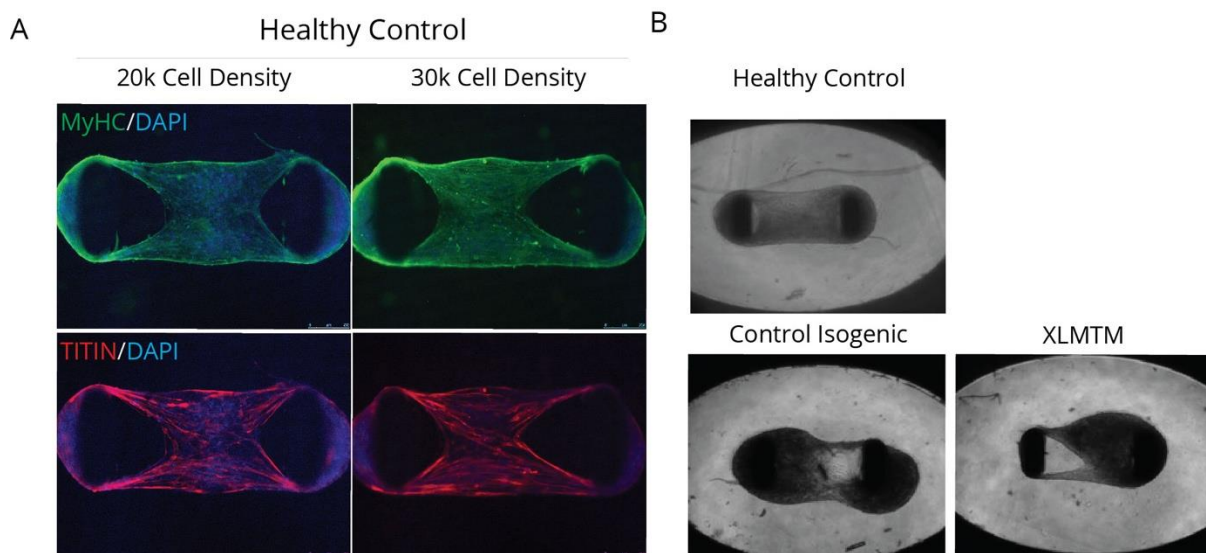


**Figure 10:** Generation of 3D muscles on MUSbit™ chip. (A) Immunofluorescence images of 3D muscles on MUSbit™ chip generated using Healthy control iPSC derived myogenic cells. Images show myofibers positive for muscle markers Myosin Heavy chain (MyHC, green) and TITIN (red). Nuclei were stained with DAPI (blue). Scale bar 250  $\mu\text{m}$ . (B) Microscopic images of the 3D single artificial skeletal muscles 2 days into differentiation.

*Figure 10*

### 3. Conclusions

Taken together, the results reported here show achievement of all goals planned in this Deliverable. We successfully generated disease-specific, multilineage 3D muscle cultures for all target diseases of our project (DMD, L-CMD, UCMD and XLCNM) whilst also developing a protocol to show formation, differentiation and maturation of 3D engineered muscle microtissues using hiPSC-derived skeletal myocytes with impaired Dystrophin expression in a DMD disease model on the MUSbit™ platform.

### References

1. Maffioletti, S.M., et al., *Three-Dimensional Human iPSC-Derived Artificial Skeletal Muscles Model Muscular Dystrophies and Enable Multilineage Tissue Engineering*. Cell Rep, 2018. **23**(3): p. 899-908.
2. Pinton, L., et al., *3D human induced pluripotent stem cell-derived bioengineered skeletal muscles for tissue, disease and therapy modeling*. Nat Protoc, 2023. **18**(4): p. 1337-1376.
3. Fernandopulle, M.S., et al., *Transcription Factor-Mediated Differentiation of Human iPSCs into Neurons*. Curr Protoc Cell Biol, 2018. **79**(1): p. e51.
4. Caron, L., et al., *A Human Pluripotent Stem Cell Model of Facioscapulohumeral Muscular Dystrophy-Affected Skeletal Muscles*. Stem Cells Transl Med, 2016. **5**(9): p. 1145-61.
5. Orlova, V.V., et al., *Generation, expansion and functional analysis of endothelial cells and pericytes derived from human pluripotent stem cells*. Nat Protoc, 2014. **9**(6): p. 1514-31.
6. Hall, C.E., et al., *Progressive Motor Neuron Pathology and the Role of Astrocytes in a Human Stem Cell Model of VCP-Related ALS*. Cell Rep, 2017. **19**(9): p. 1739-1749.